

# Effects of the addition of edible polysaccharides on the properties of soybean protein isolate gels

Chonghao Bi, Aoxue Qie, Xueying Wang, Tong Zhou, Shangyi Chi, Yi Liu, Bin Tian\*

(School of Artificial Intelligence, Beijing Technology and Business University, Beijing 100048, China)

**Abstract:** The gel properties of soybean isolate protein (SPI) gels are susceptible to the influence of other components in food products, particularly edible polysaccharides. Therefore, six common edible polysaccharides were selected in this study to investigate their effects on the rheological properties, thermal properties, and microstructure of acid-induced soybean isolate protein self-assembled gels (SPIASG). The experimental results showed that the support capacity and creep recovery of SPIASG with added polysaccharides were higher than those of the control group without added polysaccharides, and the gel with Xanthan gum (XG) was the most effective. The hybrid gel, with added Condensed resin (CR), Xanthan gum (XG), Carrageenan (CA), and CMC formed a stronger network structure. Additionally, compared with SPIASG, the hybrid gel with added edible polysaccharides the water-holding capacity of SPI hybrid gels was relatively improved. In this study, a simple and easy method was obtained to significantly improve the gel properties of SPIASG, analyzed and compared the effectiveness of various polysaccharides to enhance its gel properties, and provided some ideas to improve the gel properties of SPI protein gels.

**Keywords:** soybean protein isolate gels, self-assembled gels, edible polysaccharides, rheological properties

**DOI:** 10.25165/j.ijabe.20241703.8030

**Citation:** Bi C H, Qie A X, Wang X Y, Zhou T, Chi S Y, Liu Y, et al. Effects of the addition of edible polysaccharides on the properties of soybean protein isolate gels. *Int J Agric & Biol Eng*, 2024; 17(3): 241–248.

## 1 Introduction

Soybean protein isolate (SPI) is widely used as a kind of food ingredient in the food industry because of its functional properties of good gelation, conjugation, and emulsification. SPI can form gels through different mechanisms, including acid-induced gels, enzyme-induced gels, salt-induced gels, etc.<sup>[1]</sup>. The principle of acid-induced gels is that by lowering the pH to the isoelectric point of SPI, the electrostatic repulsion among protein molecules will be greatly reduced. The SPI will first form aggregates and clusters, then these aggregates and clusters will form a gel network<sup>[2]</sup>. The gel properties of SPIASG are susceptible to numerous factors, such as ionic strength, protein concentration, and other food components<sup>[3-5]</sup>. The addition of edible polysaccharide components not only allows the gel system to combine individual advantages of both proteins and polysaccharides but also increases the possibility of diversifying the gel structure through protein-polysaccharide interactions. The rheological properties and microstructure of the protein-polysaccharide complexes affect the choices of gel manufacturing methods and the sensory properties of the final product<sup>[1]</sup>. Accordingly, research on protein-polysaccharide interactions has become a hot topic for scholars<sup>[6-8]</sup>.

At present, scholars at home and abroad have conducted a lot of research on the addition of polysaccharides to improve the

microstructure, foaming, emulsification, rheology, water retention, and preparation of microcapsules of soy protein. Lopes-da-Silva and Monteiro<sup>[9]</sup> studied the gelling and emulsification properties of soy protein hydrolysates in the presence of neutral polysaccharides, demonstrating that under certain conditions, depending on the concentration and molecular weight of the biopolymer, the presence of non-gelling polysaccharides could improve the functional properties of soy protein hydrolysates. Wang et al.<sup>[10]</sup> studied the effect of Mesona blumes polysaccharide on the properties and microstructure of acid-induced soybean isolate gels and the research showed that the apparent viscosity and energy storage modulus of SPI-MBP gels increased significantly with the rise of Mesona blumes concentration. Wee et al.<sup>[11]</sup> studied the effect of hydrochloric acid on acid-induced soybean isolate polysaccharide gels. The results showed that with higher charge density (pH<1.2) or higher concentration of polysaccharides, denser network structures were formed among the biopolymers, resulting in faster formation and higher mechanical strength of the mixed gels. Jordana et al.<sup>[12]</sup> studied the interactions of soy protein in water-soluble soy extracts with edible polysaccharides (carrageenan (CA) and carboxymethyl cellulose) in polydextrose solutions and the research showed that both polysaccharides had a significant effect on the pH solubility profile of soy protein. Soy protein isolate and various edible polysaccharide blend systems have also been widely used in modern food systems to improve and optimize food texture. The conclusions obtained from these previous studies provide us with some ideas and theoretical basis for the coactivation of polysaccharides with acid-induced soy proteins to form gels.

However, studies on polysaccharide-protein interactions in acid-induced gels have mainly focused on the field of milk proteins. Xu et al.<sup>[13]</sup> studied the effect of okra polysaccharides on the texture and microstructure of yogurt and found that the addition of okra polysaccharides reduced the porous structure of the gel and promoted the formation of larger protein clusters, ultimately leading to a more compact protein network. The effects of different

**Received date:** 2022-11-10 **Accepted date:** 2023-04-04

**Biographies:** Chonghao Bi, Associate Professor, research interest: characterization of agricultural materials, Email: [bichonghao@btbu.edu.cn](mailto:bichonghao@btbu.edu.cn); Aoxue Qie, MS, research interest: food processing mechanisms, Email: [joy\\_4\\_qie@163.com](mailto:joy_4_qie@163.com); Xueying Wang, MS, research interest: food machinery, Email: [965631898@qq.com](mailto:965631898@qq.com); Tong Zhou, MS, research interest: characterization of agricultural materials, Email: [923615892@qq.com](mailto:923615892@qq.com); Shangyi Chi, MS, research interest: food machinery, Email: [920312701@qq.com](mailto:920312701@qq.com); Yi Liu, PhD, research interest: food processing, Email: [yiliu@btbu.edu.cn](mailto:yiliu@btbu.edu.cn).

\*Corresponding author: Bin Tian, Associate Professor, research interest: food machinery. School of Artificial Intelligence, Beijing Technology and Business University, Beijing 100048, China. Email: [tianbin@btbu.edu.cn](mailto:tianbin@btbu.edu.cn).

concentrations of dextran (DEX500) on the physical properties of acidified milk gels were investigated by Mende et al.<sup>[14]</sup> This study provides valuable insights into the improvement of texture and stability of fermented dairy products through the addition of specific polysaccharides and provides a scientific basis for the use of polysaccharides as food additives in the food industry. The main objective of the study by Daniloski et al.<sup>[15]</sup> was to investigate how structural differences in polymorphisms of  $\beta$ -casein ( $\beta$ -CN) affect the behavior of the corresponding skimmed milk in acid-induced (using gluconolactone  $\delta$ -lactone, GDL) gelation, and the results of the study provide new insights into the factors influencing the gelation properties of milk in the dairy industry. Liu et al.<sup>[16]</sup> studied the effect of Carrageenan on acid-induced gelling of whey protein aggregates. Whey protein aggregate emulsion gelation was produced by lowering the in-situ pH using GDL. The relationship between the effect of Carrageenan addition on the net charge density of proteins and pH was determined by potentiometric titration. In addition, GDL can reduce the pH value of the system to the isoelectric point, and turn the repulsive force into an attractive force between particles. Eventually, prolonged cross-linking caused the proteins to aggregate to form a gel.

To the best of our knowledge, very little literature can be found on the interaction between polysaccharides and soybean isolate protein in acid-induced gels. Through research, it was found that the polysaccharide locust bean gum played an important role in the gel system of SPIASG. However, there is no study on the effect of different types of polysaccharides on the rheological properties and microstructure of protein-polysaccharide systems. Therefore, six common edible polysaccharides were used namely Pectin (PE), Carrageenan (CA), Xanthan gum (XG), Hydroxyethyl cellulose (HEC), Carboxymethyl cellulose (CMC), and Condensed resin (CR) for this study. Previous studies have shown that all six polysaccharides are able to perform well in terms of thickening, emulsification, and gel properties, which are needed in our quest to improve the emulsification of soy protein isolate. Consequently, rheological experiments were conducted to investigate the effects of the above polysaccharides on the gelation process, and rheological properties of soybean protein isolate. Freeze-thaw experiments were also conducted to determine the freeze-thaw stability of different samples, to obtain the water-holding capacity of each sample by centrifugation, and to observe the microstructure of each sample using CLSM.

## 2 Materials and methods

### 2.1 Materials

Soybean isolate protein (protein>90%) was purchased from Shanghai Macklin Biochemical Co., Ltd., Shanghai, China. Pectin (PE) (BR grade) was purchased from Hunan Inbos Biotechnology Co., Ltd., Hunan, China. Carrageenan (CA) (BR grade) was purchased from Shanghai Yuanye Bio-Technology Co., Ltd. (Shanghai). Xanthan gum (XG) (BR grade) was purchased from Shanghai Macklin Biochemical Co., Ltd., China. Hydroxyethyl cellulose (HEC) (BR grade) was purchased from Shanghai Xin Yu Biotech Co., Ltd., China. Cydroxymethyl cellulose (CMC) (BR grade) Hunan Inbos Biotechnology Co., Ltd., China. Condensed resin (CR) was purchased from Shanghai Macklin Biochemical Co., Ltd., China. Rhodamine B (BS grade) was purchased from Shanghai Macklin Biochemical Co., Ltd., China.

### 2.2 Methods

#### 2.2.1 Preparation of samples

##### 1) Preparation of SPI stock solutions

SPI was dissolved in deionized water at 25°C. By stirring with an intelligent magnetic stirrer (ZNCL-GS, Gongyi Yuhua Instrument Co., Ltd., China) and a Cantilever stirrer (IKA MINISTAR 20, IKA Instruments Germany Ltd., Germany), a 9% (w/v) SPI solution was obtained. SPI solution was heated in a 90°C water bath for 30 min and then cooled to reach room temperature. For full hydration, the stock solution was placed into a refrigerator at 4°C overnight.

2) Preparation of polysaccharide stock solutions of the same viscosity

By using an intelligent magnetic stirrer, different types of polysaccharides were dissolved in deionized water at 25°C. The final concentrations of each polysaccharide solution were as follows: 0.015% Pectin solution, 0.045% Carrageenan solution, 0.075% Xanthan gum solution, 0.105% HEC solution, 0.21% CMC solution, and 0.048% Condensed resin solution.

##### 3) Preparation of polysaccharide-SPI mixed solutions

Different types of polysaccharide stock solution were mixed with SPI stock solution at a ratio of 1:2. By thoroughly shaking with a Vortex oscillator (Vortex-2, IKA Instruments Germany Ltd., Germany) and then standing, we obtained a mixed solution of polysaccharide-6% (w/v) SPI. The concentrations of polysaccharides in the mixed solutions were 0.005% Pectin, 0.015% Carrageenan, 0.025% Xanthan gum, 0.035% HEC, 0.07% CMC, and 0.016% Condensed resin, respectively.

##### 4) Sample preparation for rheological experiments

2% (w/v) glycono- $\delta$ -lactone (GDL) was added to the polysaccharide-SPI mixed solutions, and the GDL was completely dissolved after shaking for 1 min with a Vortex oscillator and standing for 1 min to allow air bubbles to escape.

##### 5) Sample preparation for microstructure and fractal analysis

2% GDL and 0.01% (v/v) rhodamine B stain were added to the polysaccharide-SPI mixed solutions. After shaking for one minute with a Vortex oscillator, a drop of mixed solutions was dropped into a confocal small dish container and left to stand for 60 min at room temperature with tinfoil masking

##### 6) Sample preparation for thermal stability experiments

2% GDL was added to the polysaccharide-SPI mixed solutions. After shaking for one minute with a Vortex oscillator, the solutions were subsequently left to freeze-dry for 24 h. About 2 mg samples were precisely weighed and the samples were pressed by using a flat aluminum crucible.

##### 7) Sample preparation for gel water retention experiments

2% GDL was added to the polysaccharide-SPI mixed solutions. After shaking for one minute with a vortex oscillator, the solutions were left to stand for 60 min at room temperature.

#### 2.2.2 Rheological tests

The rheological tests were done with a rotational rheometer (DHR-2, TA Instrument Company, New Castle, DE, USA). An aluminum plate clamp with a diameter of 40mm was chosen. The distance between the fixture and the Peltier plate connected to the circulating cooling system was 1000  $\mu$ m. The sample prepared for rheological experiments was transferred between the Peltier plate and the fixture after the distance between the fixture and the Peltier plate was adjusted. The excess sample was scraped away with a squeegee, and a thin layer of low-viscosity silicone oil was applied on the edge of the sample exposed to air to prevent moisture evaporation due to high temperature.

##### 1) Time sweep tests

Time scan tests were performed at a temperature of 60°C and a constant frequency of 1 Hz throughout the gel formation process,

and the energy storage modulus ( $G'$ ) was recorded. On the basis of the strain scan tests, an angular frequency of 6.283 rad/s and a strain amplitude of 1% in the time scan tests were selected to make sure the strain amplitude of all samples remained within the linear viscoelastic region. The changes in the parameters such as dynamic modulus (energy storage modulus  $G'$ ; loss modulus  $G''$ ) of the mixed system was measured by time.

The trend of the energy storage modulus  $G'$  of the polysaccharide-SPI acid-induced mixed gel with time  $t$  conforms to the following kinetic equation (Equation (1)):

$$G'(t) = G'_{\infty} [1 - e^{-K(t-t_g)}] \quad (1)$$

where,  $G'_{\infty}$  denotes the highest value that the energy storage modulus  $G'$  (Pa) can reach, Pa;  $K$  is the empirical reaction rate constant,  $s^{-1}$ ;  $t_g$  denotes the onset time of gel formation, s;  $t$  denotes the time variable, s.

#### 2) Frequency sweep tests

Frequency scan experiments were performed at 25°C in a range of angular frequencies of 0.1-10.0 rad/s. Storage modulus, loss modulus, and loss angle tangent values were recorded.

The correlation between  $G'$  and  $G''$  and frequency  $\omega$  (rad) of polysaccharide-SPI acid-induced mixed gels conforms to the following power-law functions (Equations (2) and (3)):

$$G' = K' \omega^{n'} \quad (2)$$

$$G'' = K'' \omega^{n''} \quad (3)$$

where,  $K'$  and  $K''$  denote the power law constants, which are the storage and loss modulus at 1 rad/s, respectively, Pa;  $n'$  and  $n''$  denote the frequency index and the value indicates the frequency dependence of the storage modulus  $G'$  (Pa) and loss modulus  $G''$  (Pa).

#### 3) Creep/recovery tests

Creep recovery experiments were performed by applying an instantaneous shear stress of 7.9775 Pa to the polysaccharide-SPI acid-induced mixed gels at a temperature of 25°C, and the strain (%) and compliance  $J$  ( $\text{Pa}^{-1}$ ) of the samples were recorded.

The creep flexibility curves of the polysaccharide-SPI acid-induced mixed gels conform to the following four-element Maxwell-Voigt model (Equations (4) and (5)):

$$J(\omega) = \frac{1}{G_H} + \frac{1}{G_V} \left(1 - e^{-\frac{t}{\tau}}\right) + \frac{1}{\eta_N} \quad (4)$$

$$\tau = \frac{\eta_V}{G_V} \quad (5)$$

where,  $J$  represents the flexibility, which is numerically equal to the strain divided by the stress,  $\text{Pa}^{-1}$ ;  $G_H$  and  $G_V$  represent the elastic modulus of the Hook element and the Voigt element, Pa, respectively;  $\tau$  is the hysteresis time, s;  $\eta_V$  and  $\eta_N$  represent the viscous part of the Voigt element ( $\text{Pa}\cdot\text{s}$ ) and the viscous part of the Newtonian element ( $\text{Pa}\cdot\text{s}$ ), respectively.

#### 2.2.3 Microstructure and fractal analysis

The confocal laser scanning microscope (CLSM) (TCS-SP8, Leica, Germany Ltd., Germany) was used to observe and acquire microstructure images of polysaccharide-SPI acid-induced mixed gels. In the confocal laser scanning microscopy test, the CLSM was equipped with an inverted microscope (Leica DMI6000) and a He-Ne/visible laser source. An objective lens of 40 by 0.85 (NA) was used to observe and acquire images. The fractal parameters of the polysaccharide-SPI acid-induced mixed gels were calculated by using the images taken from CLSM. The RGB images of 1024 by 1024 pixels were converted to 8-bit gray images. Black and white

binarization was performed based on the middle value of the gray level histogram of each image as a threshold<sup>[17]</sup>. The Box-counting method was applied to calculate the fractal dimension ( $D_f$ ) of the polysaccharide-SPI acid-induced mixed gels. The method is based on the scaling model given by Equations (6) and (7).

$$D_p = -\frac{\log N_{\varepsilon}}{\log \varepsilon} \quad (6)$$

$$D_f = D_p + 1 \quad (7)$$

where,  $N_{\varepsilon}$  is the number of boxes at a certain scale containing part of the image;  $\varepsilon$  is the corresponding scale. The determination of  $D_f$  by image analysis is based on a two-dimensional space. Therefore, when it comes to a three-dimensional (3D) space of the gel features, an addition of an extra dimension to the  $D_p$  value is required. where  $D_p$  is Box-counting fractal dimension.

#### 2.2.4 Thermal stability tests

Differential scanning calorimeters (DSC250, TA Instrument Company, NEW CASTLE, DE, USA) were used for thermal stability testing. The initial scanning temperature was set at 40°C and ramped up to 200°C at 20°C/min. The variation of thermal power in different temperatures was analyzed to study the thermal stability of polysaccharide-SPI acid-induced mixed gels.

#### 2.2.5 Water-holding gel tests (WHC)

A centrifuge was used in the gel water-holding experiments at 500 r/min and 1000 r/min, and the weight before the experiments was recorded to ensure that the weight error between each group of samples would not exceed 0.5 g. Afterwards, the water precipitated was filtered through filter paper for 20 min and then weighed again. The data were recorded and analyzed.

The gel water holding rate is calculated by Equation (8).

$$\text{WHC} = \frac{M_i - M_w}{M_i} \times 100\% \quad (8)$$

where,  $M_i$  is the weight of the gel before centrifugation, g;  $M_w$  is the weight of water released from the gel after centrifugation, g.

#### 2.2.6 Data analysis

Data were processed in SPSS software (SPSS Statistics 22.0), and one-way analysis of variance and Duncan's test were applied to analyze significant differences ( $p < 0.05$ ). At least three parallel experiments were conducted for each experiment, and the results were presented as mean  $\pm$  standard deviation.

## 3 Results and discussion

### 3.1 Time sweep tests

The trend of the energy storage modulus  $G'$  of the polysaccharide-SPI acid-induced mixed gels with time  $t$  is shown in Figure 1. In Figure 1, it can be seen that the polysaccharide-SPI acid-induced mixed gels have similar gel formation trends to the acid-induced SPI gels, which may be explained by the dominant role of the ionization degree of the charged groups of polysaccharides and proteins during the formation of polysaccharide-protein condensates<sup>[8]</sup>.  $G'$  approaches 0 during the initial period of the gel, and then rises rapidly. This is due to the accelerated dissociation of the acid inducer GDL at a higher temperature and the decrease of the pH of the system to reach the isoelectric point of SPI to generate a strong enough electrostatic attraction to form polysaccharide-SPI gels<sup>[17]</sup>. It can be seen that the addition of polysaccharides has a significant effect on the trend of the overall gel curve, the rate of  $G'$  rise, and the height of the final plateau period. To quantify the effect of various polysaccharides on polysaccharide-SPI acid-induced mixed gel formation, a nonlinear regression of the gel curves was

performed by using a one-level kinetic model as described in 2) in Section 2.2.2 ( $R^2 \geq 99.5\%$ ).

The  $G'_\infty$ ,  $K$ , and  $t_g$  of the polysaccharide-SPI acid-induced mixed gels formed by different polysaccharides are listed in Table 1. It can be seen that the  $G'_\infty$  values increase significantly with the addition of polysaccharides, and the  $G'_\infty$  of Xanthan gum is the largest, reaching 2046.541 Pa, which is 6.8 times higher than that of the acid-induced SPI gels. This result indicates that the addition of polysaccharides can increase the elastic strength of the gel. This may be caused by the interaction between SPI and polysaccharides to form a homogeneous complex network<sup>[8]</sup>. The table also shows that Carrageenan contributes the least to the increase in  $G'_\infty$  of the polysaccharide-SPI acid-induced mixed gels, followed by Pectin, CMC, and Condensed resin, with the largest contribution from HEC.

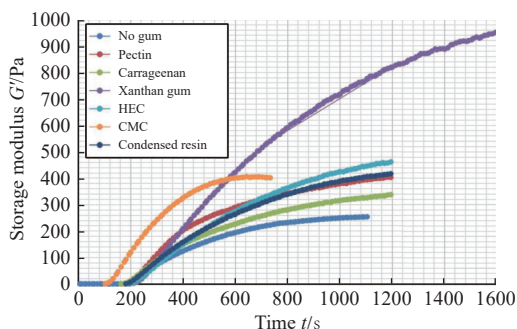


Figure 1 Variation of energy storage modulus  $G'$  of mixed gels with time  $t$

Table 1 Parameters of the first-order dynamic equation of mixed gel formation curve

Polysaccharide	$G'_\infty/\text{Pa}$	$K/\text{s}^{-1}$	$t_g/\text{s}$	$R^2/\%$
No gum	300±72 <sup>a</sup>	0.003 <sup>a</sup>	189.45±0.79 <sup>a</sup>	100.0%
Pectin/SPI-AG	372±56 <sup>b</sup>	0.004 <sup>a</sup>	205.39±1.89 <sup>b</sup>	99.9%
Carrageenan/SPI-AG	341±75 <sup>c</sup>	0.003 <sup>a</sup>	188.15±1.67 <sup>a</sup>	100.0%
Xanthan gum/SPI-AG	2047±283 <sup>d</sup>	0.001 <sup>e</sup>	224.54±3.07 <sup>c</sup>	99.9%
HEC/SPI-AG	675±94 <sup>e</sup>	0.001 <sup>e</sup>	214.22±2.02 <sup>c</sup>	99.9%
CMC/SPI-AG	431±85 <sup>b</sup>	0.006 <sup>b</sup>	148.44±4.57 <sup>d</sup>	99.6%
Condensed resin/SPI-AG	497±97 <sup>b</sup>	0.002 <sup>ac</sup>	198.91±0.95 <sup>b</sup>	100.0%

As listed in Table 1, the  $K$  values of the polysaccharide-SPI acid-induced mixed gels with the addition of Pectin, Carrageenan, and Condensed resin are not significantly different from those of the acid-induced SPI gels, which indicates that the addition of these polysaccharides has little effect on the rate of polysaccharide-SPI acid-induced mixed gel formation. However, the  $K$  values of the polysaccharide-SPI acid-induced mixed gels with the addition of Xanthan gum and HEC are significantly lowered, which indicates that the addition of these two polysaccharides has a significant slowing effect on the rate of the mixed gel gelation reaction, and interestingly, these two polysaccharides also happen to be the polysaccharides that increase the elastic strength of the gels the most. This can be caused by the addition of polysaccharides, which lead to an increase in the viscosity of the solution. This means that the rate of decrease in pH is slowed down, which gives SPI more opportunities to form three-dimensional network binding sites. More specifically, the addition of CMC significantly increases the gelation rate, this may be because the concentration of CMC is the highest among polysaccharides with the same viscosity, the more

CMC molecules adsorbs on the surface of SPI, the lower the pH point where SPI aggregates with each other, and the rate of gelation increases. However, it does not correspondingly decrease the gel strength of the mixed gels.

It can be seen that the  $t_g$  of polysaccharide-SPI acid-induced mixed gels with the addition of Carrageenan does not change significantly, and the gel formation time does not change much compared with the acid-induced SPI gels, while the  $t_g$  of polysaccharide-SPI acid-induced mixed gels with the addition of Pectin, Condensed resin, Xanthan gum, and HEC increases significantly, indicating that the addition of these polysaccharides delays the onset of gel formation and the addition of Xanthan gum and HEC causes more time delay to the gel formation. The  $t_g$  of polysaccharide-SPI acid-induced mixed gels with the addition of CMC is significantly decreased, indicating that the addition of CMC brings earlier gel formation.

### 3.2 Frequency sweep tests

The curves of the modulus of the polysaccharide-SPI acid-induced mixed gels with the angular frequency with the addition of different polysaccharides are shown in Figure 2. It can be seen that the energy storage modulus is much higher than the loss modulus at the same frequency, indicating that all mixed gels exhibit distinct solid properties<sup>[8]</sup>. With the increase of frequency, the polysaccharide-SPI acid-induced mixed gels with Xanthan gum added had a more significant increase in storage modulus  $G'$  and loss modulus  $G''$  than the other five groups of samples. This is probably because the addition of Xanthan gum leads to an increase in the gel formation time, and the formed 3D gel network is stronger. This indicates that the addition of Xanthan gum polysaccharide changed the overall frequency dependence of the gel. All gels exhibit viscoelasticity at high frequencies.

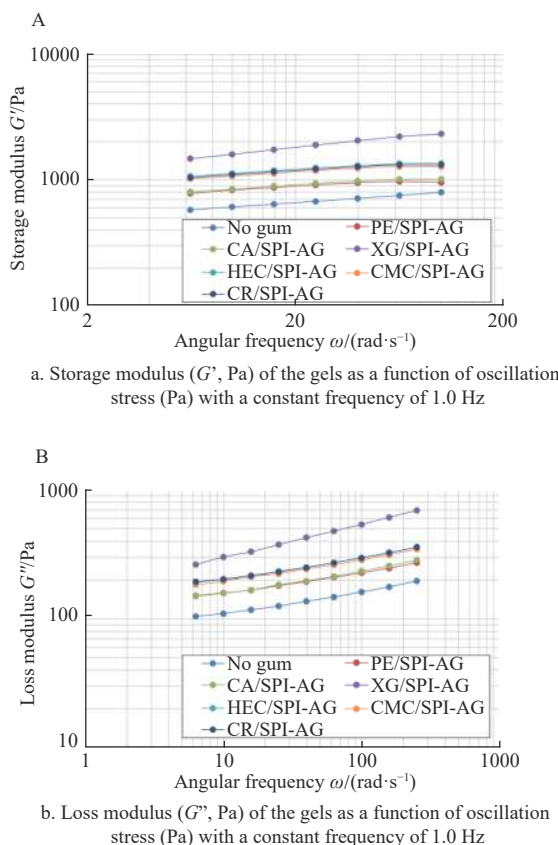


Figure 2 Trends of storage modulus and loss modulus of mixed gels with the applied oscillation frequency

The effect of fitting the power-law function of polysaccharide-SPI acid-induced mixed gels with the addition of different polysaccharides of the same viscosity is listed in Table 2. The  $K'$  values of the samples without polysaccharide addition are much

smaller than that of the other six groups, indicating that the addition of polysaccharide increases the strength of the gels. This may be explained by the fact that polysaccharides behave as active packing particles dispersed in the viscoelastic protein network<sup>[18]</sup>.

**Table 2** Variation of frequency power law parameters for the mixed gels

Polysaccharide	$G' = k' \cdot \omega^{\alpha'}$			$G'' = k'' \cdot \omega^{\alpha''}$			tan $\delta$
	$K'/\text{Pa}$	$n'$	$R^2/\%$	$K''/\text{Pa}$	$n''$	$R^2/\%$	
No gum	346.123±26.359 <sup>a</sup>	0.211±0.002 <sup>ab</sup>	99.8%	24.079±7.225 <sup>a</sup>	0.517±0.079 <sup>a</sup>	99.5%	0.592
Pectin/SPI-AG	607.365±34.739 <sup>ab</sup>	0.123±0.17 <sup>a</sup>	99.1%	36.147±11.944 <sup>b</sup>	0.501±0.087 <sup>a</sup>	99.3%	0.754
Carrageenan/SPI-AG	569.183±20.083 <sup>ab</sup>	0.153±0.01 <sup>a</sup>	99.2%	38.646±8.553 <sup>b</sup>	0.486±0.058 <sup>a</sup>	99.9%	0.685
Xanthan gum/SPI-AG	707.823±48.198 <sup>b</sup>	0.307±0.02 <sup>b</sup>	99.5%	39.191±10.71 <sup>b</sup>	0.702±0.071 <sup>b</sup>	99.7%	0.563
HEC/SPI-AG	756.106±22.696 <sup>b</sup>	0.154±0.009 <sup>a</sup>	99.7%	47.266±11.585 <sup>c</sup>	0.497±0.067 <sup>a</sup>	99.8%	0.690
CMC/SPI-AG	730.289±25.284 <sup>b</sup>	0.148±0.001 <sup>a</sup>	99.2%	50.066±11.585 <sup>c</sup>	0.471±0.061 <sup>a</sup>	99.6%	0.686
Condensed resin/SPI-AG	746.291±24.915 <sup>b</sup>	0.151±0.010 <sup>a</sup>	99.4%	47.801±12.678 <sup>c</sup>	0.494±0.070 <sup>a</sup>	99.1%	0.694

Note: Different superscripts a, b, and c indicate significant differences ( $p > 0.05$ ).

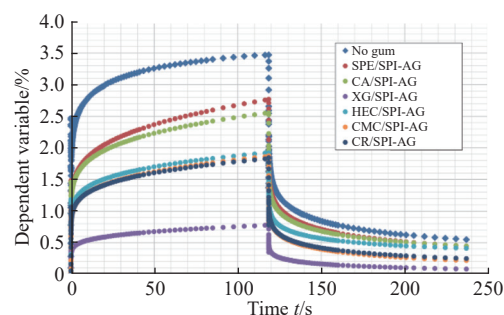
As can be seen from the table, the frequency dependence is slight in the gels except for the addition of Xanthan gum, showing the time-stability of the gel networks. And the relative increase of  $n''$  vs  $n'$  has been augmented after adding polysaccharides. Specifically for Xanthan gum (128%). This effect indicates a gel reinforcing when polysaccharide is added. The  $n''$  is higher than  $n'$  it can be deduced that there is a shear-induced gelation at lower frequencies since the rate of decrease in  $G''$  is higher than that of  $G'$ . At the same time, the value of tan $\delta$  is increased except for the addition of Xanthan gum, which indicates a higher gel elasticity (lower tan $\delta$ ) with the addition of Xanthan gum. This is probably because Xanthan gum is a non-curdlan, which has strong hydrophilicity. After adding Xanthan gum, SPI, and Xanthan gum form a semi-interpenetrating gel network. In the SPI system, the attraction between protein molecules may be promoted through the volume repulsion effect, and the arrangement of protein molecules is promoted by reducing the chance of protein molecules contacting the surrounding solution.

### 3.3 Creep-recovery tests

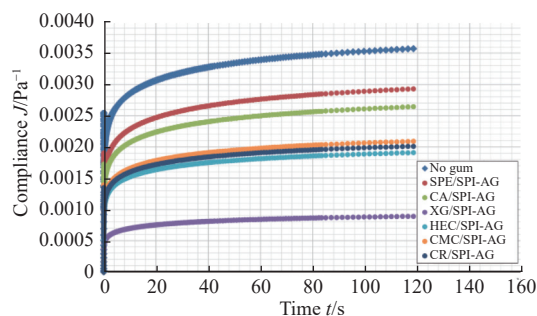
The variation curves of the strain of the polysaccharide-SPI acid-induced mixed gels with the same viscosity and different polysaccharides as a function of time are shown in Figure 3a. With the increase of time, the strain rises gradually, then drops abruptly at the moment of reaching the highest point, and then decreases gradually to a stable value. The maximum creep value (i.e., the peak strain at the end of creep) is in descending order: polysaccharide-SPI acid-induced mixed gel with Pectin, Carrageenan, HEC, CMC, Condensed resin, and Xanthan gum. A higher peak strain indicates a softer structure, stronger flow ability, lower ability to recover after gel deformation, and lower rigidity of gel structure<sup>[19]</sup>. This is probably because hydrogen bonding and hydrophobic interactions are the main driving forces for Pectin aggregation, and under acidic conditions, unesterified carboxyl groups exist as ionized salts, which lead to repulsion between negative charges, reducing the attraction between Pectin and water molecules, which hinders Pectin from forming a network, so the mixed gel structure with Pectin addition is softer.

The curves of the flexibility of the polysaccharide-SPI acid-induced mixed gels with the addition of different polysaccharides of the same viscosity over time are shown in Figure 3b. With the increase of time, the flexibility increases and then tends to a stable peak, and the peak of the polysaccharide-SPI acid-induced mixed gels with the addition of Pectin is the largest, followed by Carrageenan, CMC, Condensed resin, and HEC. The peaks of the last three are not significantly different. The peak of the polysaccharide-SPI acid-induced mixed gel with the addition of

Xanthan gum remains the last. It can be seen that the addition of polysaccharides can lead to the formation of stronger network structures.



a. Creep recovery curves of different gels at an instantaneous stress of 7.9775 Pa



b. Variation of flexibility with time for different gels at an instantaneous stress of 7.9775 Pa

Figure 3 Recovery curve of creep of mixed gels

The effects of the Maxwell-Voigt model fitting for different types of polysaccharide-SPI acid-induced mixed gels with the same viscosity are listed in Table 3, and the order of  $G_H$  in descending order is added HEC, Pectin, No gum, Condensed resin, Xanthan gum, Carrageenan, and CMC. Among them, there is no significant difference in  $G_H$  in the first three samples, samples with added Carrageenan and samples with Xanthan gum. This suggests that the addition of Carrageenan, CMC, Xanthan gum, and Condensed resin leads to a lower or slowed transient elastic behavior of the polysaccharide-SPI acid-induced mixed gels, among which the addition of CMC has the most significant effect on the gels.

The order of  $G_V$  from the largest to the smallest is consistent with  $G_H$ , respectively, where there is no significant difference in  $G_V$  between the first three samples and the last three samples. Interestingly, the order of  $G_H$  and  $G_V$  size arrangement shows an opposite order of the maximum creep value in Figure 3, indicating

that the elastic modulus is negatively correlated with the maximum creep value. The order of  $\eta_N$  in descending order is HEC, no gum, Pectin, Condensed resin, CMC, Xanthan gum, and Carrageenan. Among them, there is no significant difference in  $\eta_N$  between the first three samples, and the samples with CMC and Xanthan gum added. The last four samples showed a significant decrease in  $\eta_N$ . The values of  $G_V$  and  $\eta_V$  are related to the stiffness and viscous orientation of the amorphous polymer chains over a short period<sup>[19]</sup>.

These trends suggest that the addition of Carrageenan, Xanthan gum, CMC, and Condensed resin enhances the orientation of the gel matrix, increases the probability of linkage between molecular chains, and forms a stronger network structure<sup>[20]</sup>.

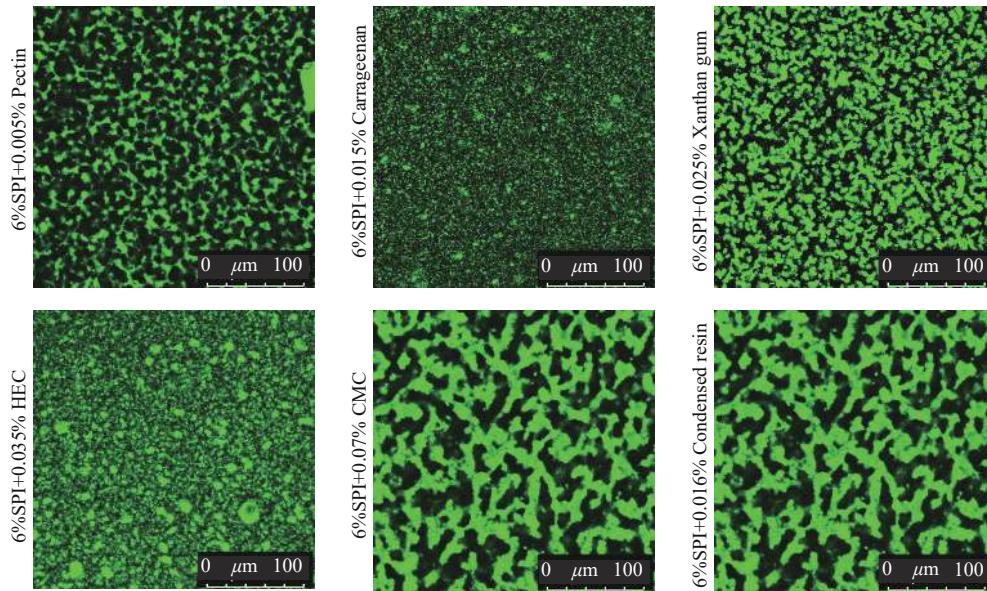
**3.4 Microstructure and fractal analysis**

The microstructures of different kinds of polysaccharide-SPI acid-induced mixed gels with the same viscosity are shown in Figure 4a. The colored region in the image is the SPI in the system

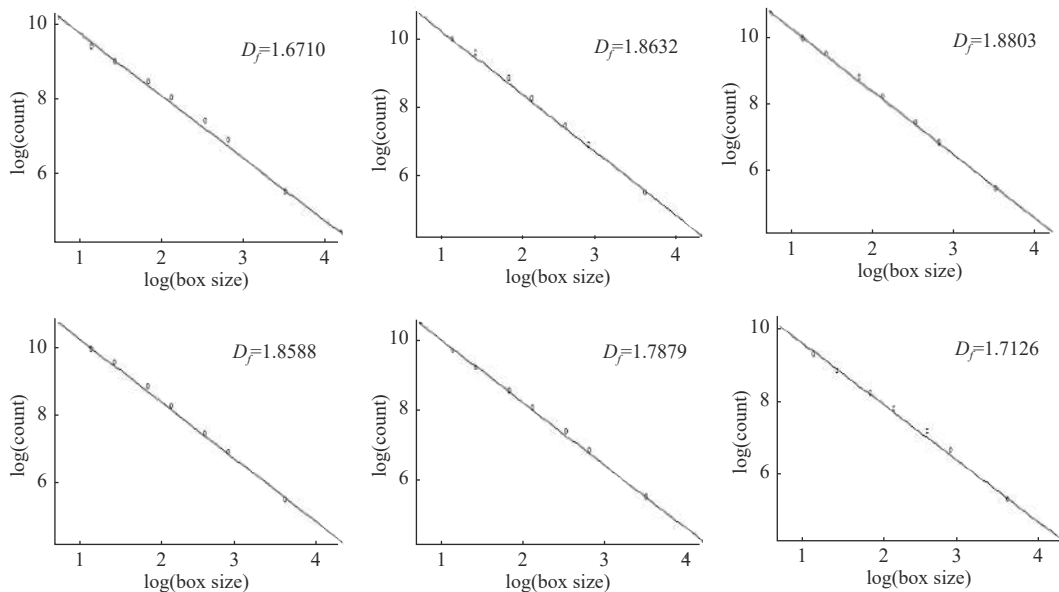
**Table 3 Variation of Maxwell-Voigt model parameters for the mixed gels**

Polysaccharide	$G_H$ /Pa	$G_V$ /Pa	$\tau$ /s	$\eta_N$ /Pa·s	$R^2$ /%	$\eta_V$ /Pa·s
No gum	78.566±0.389 <sup>a</sup>	198.289±2.098 <sup>a</sup>	9.154±0.376 <sup>a</sup>	33 569.87±1240.87 <sup>a</sup>	99.4%	1815.138
Pectin/SPI-AG	79.239±0.374 <sup>a</sup>	192.584±2.701 <sup>a</sup>	9.101±0.330 <sup>a</sup>	32 336.69±1130.70 <sup>a</sup>	99.7%	1752.707
Carrageenan/SPI-AG	36.207±0.180 <sup>bc</sup>	84.921±1.212 <sup>b</sup>	9.095±0.336 <sup>a</sup>	14 281.040±509.176 <sup>b</sup>	99.7%	772.356
Xanthan gum/SPI-AG	41.148±0.211 <sup>b</sup>	96.25±1.46 <sup>b</sup>	9.387±0.365 <sup>a</sup>	15 312.370±552.057 <sup>bc</sup>	99.7%	903.499
HEC/SPI-AG	79.927±0.315 <sup>a</sup>	200.684±2.927 <sup>a</sup>	9.137±0.344 <sup>a</sup>	35 630.520±1371.207 <sup>a</sup>	99.7%	1833.650
CMC/SPI-AG	31.1119±0.144 <sup>c</sup>	88.805±1.388 <sup>b</sup>	8.828±0.359 <sup>a</sup>	16 797.740±731.659 <sup>bc</sup>	99.6%	788.971
Condensed resin/SPI-AG	42.863±0.195 <sup>b</sup>	112.977±1.666 <sup>c</sup>	9.149±0.348 <sup>a</sup>	21 405.86±889.38 <sup>c</sup>	99.6%	1033.627

Note: Different superscripts a, b, and c indicate significant differences ( $p > 0.05$ ).



a. CLSM images



b. Corresponding fractal analysis

Figure 4 Microstructure of gels with different added polysaccharides

stained by Rhodamine B, while the polysaccharide does not stain and is the black region in the image. The experimental results show that with the addition of different kinds of edible gums, different morphologies are shown in the protein-enriched regions. The SPI in the gels with the addition of Carrageenan and HEC shows oil-drop-like aggregation, and the rest of the edible gums show phase separation from the proteins at different levels. Because of the low mixing entropy of polysaccharide-SPI solutions, in most cases, polysaccharides are incompatible with proteins<sup>[6]</sup>. It can be seen that the addition of polysaccharides can change the microstructure of acid-induced SPI gels to a large extent.

The effect of fractal dimension of different types of polysaccharide-SPI acid-induced mixed gels with the same viscosity is shown in Figure 4b. The fractal dimension is an important indicator to characterize the disorder and complexity of the non-homogeneous colloidal network structure<sup>[6]</sup>. So, the higher fractal dimension is usually associated with greater connectivity in the gel network (less porous matrix). As shown in the figure, 6% soybean isolate+0.025% Xanthan gum has the highest fractal dimension value of 1.8803, while 6% soybean isolate+0.005% Pectin has the lowest fractal dimension value of 1.6710. As listed in Table 2, the relative difference between  $n''$  and  $n'$  is 128%. Moreover,  $\tan\delta''/K' = 0.0554$  was the lowest, indicating a greater lifetime of bonds in the gel network, which is consistent with the highest  $D_f$ . From the above, it is clear that the mixed gels with the addition of Xanthan gum have the most disordered complex network structure. That is probably because Pectin, Carrageenan, HEC, CMC, and Condensed resin belong to curdlan, which mainly forms interpenetrating network gel with SPI. However, Xanthan gum is a non-curdlan, and it forms a semi-interpenetrating network gel with SPI. Therefore, in the mixed gel with the addition of Xanthan gum, the polysaccharide will be entangled in the three-dimensional network of the protein, resulting in a more complex structure of the mixed gel.

### 3.5 Thermal stability tests

The effect of temperature on heat flow for different types of polysaccharide-SPI acid-induced mixed gels with the same viscosity is shown in Figure 5. The differential calorimetric scanning test

mainly detects the heat absorption and exotherm of the lyophilized gel powder in a temperature range of 50°C-200°C. As can be seen in the figure, with the increase of the heat flow, each curve has two heat absorption peaks of approximately 0.67-0.99 W/g and 0.66-0.78 W/g. The two heat absorption peaks of around 90°C and 160°C are both protein heat absorption peaks. Specifically, the first one is the heat absorption peak of protein denaturation and the second one is the heat absorption peak of protein phase transition (from glassy to viscous flow state).

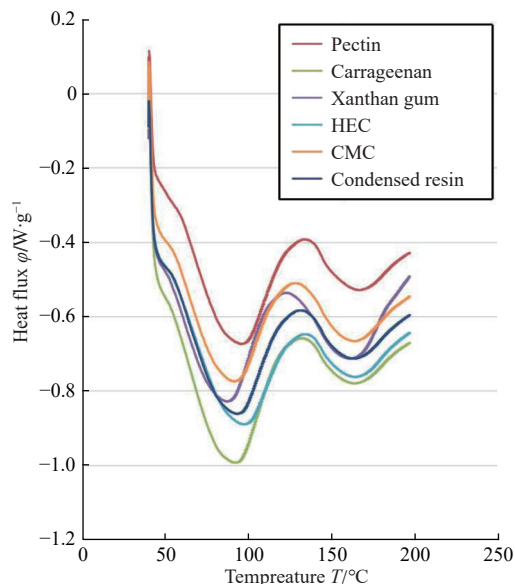


Figure 5 Variation of the heat flow rate of the mixed gels at a heating rate of 20°C/min with temperature  $T$

The effects of thermal tests of different types of polysaccharide-SPI acid-induced mixed gels at the same viscosity are listed in Table 4. According to the table, the values of all solutions do not change much. From the enthalpy analysis, we have obtained a negative result: the thermal stability of the proteins is not significantly affected by the different edible gels.

Table 4 Effect of enthalpy and peak temperature  $T_m$  corresponding to each exothermic peak in the DSC curve of the mixed gels

Polysaccharide	Enthalpy 1/J·g <sup>-1</sup>	Minimum value 1		Enthalpy 2/J·g <sup>-1</sup>	Minimum value 2	
		T/°C	Heat flux/W·g <sup>-1</sup>		T/°C	Heat flux/W·g <sup>-1</sup>
Pectin/SPI-AG	16.477±0.307 <sup>a</sup>	95.523±1.792 <sup>bc</sup>	-0.674±0.025 <sup>a</sup>	4.094±0.033 <sup>c</sup>	166.048±0.698 <sup>a</sup>	-0.731±0.010 <sup>b</sup>
Carrageenan/SPI-AG	16.481±0.174 <sup>a</sup>	98.446±1.751 <sup>ab</sup>	-0.990±0.032 <sup>c</sup>	4.102±0.086 <sup>c</sup>	164.042±0.454 <sup>c</sup>	-0.780±0.043 <sup>b</sup>
Xanthan gum/SPI-AG	14.246±0.468 <sup>d</sup>	86.091±0.772 <sup>d</sup>	-0.827±0.008 <sup>b</sup>	4.982±0.090 <sup>a</sup>	163.686±1.132 <sup>c</sup>	-0.713±0.010 <sup>b</sup>
HEC/SPI-AG	15.344±0.080 <sup>b</sup>	99.482±1.998 <sup>a</sup>	-0.886±0.012 <sup>bc</sup>	4.059±0.038 <sup>c</sup>	163.574±0.307 <sup>ab</sup>	-0.728±0.016 <sup>b</sup>
CMC/SPI-AG	14.572±0.110 <sup>cd</sup>	89.776±0.982 <sup>c</sup>	-0.772±0.028 <sup>ab</sup>	4.789±0.193 <sup>a</sup>	163.374±0.523 <sup>bc</sup>	-0.666±0.003 <sup>a</sup>
Condensed resin/SPI-AG	15.065±0.047 <sup>bc</sup>	92.008±0.967 <sup>c</sup>	-0.860±0.095 <sup>ab</sup>	4.377±0.018 <sup>b</sup>	163.096±0.403 <sup>bc</sup>	-0.713±0.019 <sup>ab</sup>

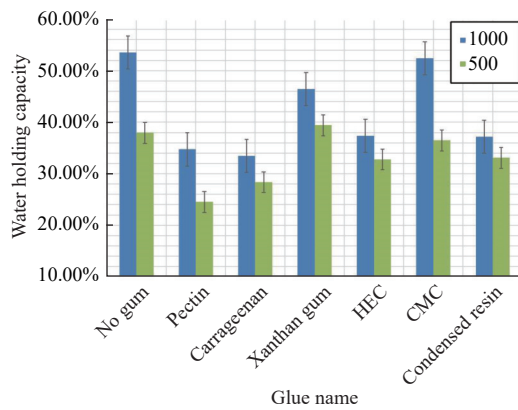
Note: Different superscripts a, b, c, and d indicate significant differences ( $p > 0.05$ ).

### 3.6 Water-holding gel tests (WHC)

The effects of gel water retention of different polysaccharide-SPI acid-induced mixed gels with the same viscosity are shown in Figure 6. At 500 r/min, the highest gel WHC is observed for SPI-AG Pectin, and the lowest gel WHC is observed for SPI-AG Xanthan gum. At 1000 r/min, the highest gel WHC is obtained with SPI-AG Carrageenan, and the lowest gel WHC is obtained with No gum.

Therefore, the experimental results show that the mixed gels with the addition of Xanthan gum have the strongest gel strength but the WHC is not the best. At 500 r/min, almost all acid-induced

gels with added polysaccharides except SPI-AG Xanthan gum have better WHC than the gels without added edible gum. At 1000 r/min, all acid-induced gels with added polysaccharides have better WHC than the gels without added edible gum, which is consistent with our usual perception that edible polysaccharides have strong water absorption. All acid-induced gels with added polysaccharides increase the WHC by more than 500 r/min. This phenomenon may be because the addition of edible polysaccharides increases the strength of the acid-induced gel and improves the water retention of the system.



Note: 500 and 1000 in legend represent different centrifugal speeds ( $r/min$ ), i.e., different centrifugal strengths.

Figure 6 Effects of different kinds of polysaccharides and soybean protein isolates on the hydrocolloid properties of gels with the same viscosity

#### 4 Conclusions

In this study, the influence of various polysaccharides on the properties of acid-induced SPIASG was examined. The results from rheological experiments indicate that the incorporation of edible polysaccharides enhances the elastic strength of the gel. This enhancement could be attributed to the development of a more uniform composite network structure between SPI and polysaccharides. Most notably, the low entropy of mixing in polysaccharide-SPI solutions suggests an inherent incompatibility between polysaccharides and proteins in many cases. Interestingly, the different edible gels tested demonstrated minimal impact on the thermal stability of the proteins. However, the introduction of polysaccharides notably increased the water-holding capacity of the gels. This effect may be linked to the ability of polysaccharides to strengthen acid-induced gels. In conclusion, this research offers insights for enhancing the structural properties, freeze-thaw stability, and water-holding capacity of gels by exploring the diverse impacts of polysaccharides. By understanding how various polysaccharides affect gel properties, it is possible to develop gels with improved structures that can find applications across various industries.

#### Acknowledgements

This work was financially supported by the 2021 Postgraduate Research Ability Improvement Program BTBU, the Joint Program of Beijing Natural Science Foundation Committee and Beijing Education Committee (Grant No. KZ201810011017), and Beijing Excellent Talent Training Project (Grant No. 2017000020124G100).

#### [References]

[1] Chang Y Y, Li D, Wang L J, Bi C H, Adhikari B. Effect of gums on the

- rheological characteristics and microstructure of acid-induced SPI-gum mixed gels. *Carbohydrate Polymers*, 2014; 108(12): 183–191.
- [2] Cavallieri A L F, da Cunha R L. The effects of acidification rate, pH and aging time on the acidic cold set gelation of whey proteins. *Food Hydrocolloids*, 2008; 22(3): 439–448.
- [3] Li A, Gong T, Yang X, Guo Y R. Interpenetrating network gels with tunable physical properties: Glucono- $\delta$ -lactone induced gelation of mixed Alg/gellan sol systems. *International Journal of Biological Macromolecules*, 2020; 151: 257–267.
- [4] Klost M, Brzeski C, Drusch S. Effect of protein aggregation on rheological properties of pea protein gels. *Food Hydrocolloids*, 2020; 108: 106036.
- [5] Lavoisier A, Aguilera J M. Starch gelatinization inside a whey protein gel formed by cold gelation. *Journal of Food Engineering*, 2019; 256: 18–27.
- [6] Yang Z, Yang H, Jiang Z W, Huang X, Li H B, Li A M, Cheng R S. A new method for calculation of flocculation kinetics combining Smoluchowski model with fractal theory. *Colloids and Surfaces A: Physicochemical and Engineering Aspects*, 2013; 423: 11–19.
- [7] Liu P C, Xu H L, Zhao Y, Yang Y Q. Rheological properties of soy protein isolate solution for fibers and films. *Food Hydrocolloids*, 2017; 64: 149–156.
- [8] Yang X, Li A Q, Li D, Guo Y R, Sun L J. Applications of mixed polysaccharide-protein systems in fabricating multi-structures of binary food gels. *Trends in Food Science & Technology*, 2021; 109: 197–210.
- [9] Lopes-da-Silva J A, Monteiro S R. Gelling and emulsifying properties of soy protein hydrolysates in the presence of a neutral polysaccharide. *Food Chemistry*, 2019; 294: 216–223.
- [10] Wang W J, Jiang L, Ren Y M, Shen M Y, Xie J H. Characterizations and hepatoprotective effect of polysaccharides from *s* against tetrachloride-induced acute liver injury in mice. *International Journal of Biological Macromolecules*, 2019; 124: 788–795.
- [11] Wee M S M, Yusoff R, Lin L, Xu Y Y. Effect of polysaccharide concentration and charge density on acid-induced soy protein isolate-polysaccharide gels using HCl. *Food Structure*, 2017; 13: 45–55.
- [12] Jordana C S, Marczak L D F, Tessaro I C, Cardozo N S M. Interactions between soy protein from water-soluble soy extract and polysaccharides in solutions with polydextrose. *Carbohydrate polymers*, 2015; 134: 119–127.
- [13] Xu K, Guo M M, Du J H, Zhang Z H. Okra polysaccharide: Effect on the texture and microstructure of set yoghurt as a new natural stabilizer. *International Journal of Biological Macromolecules*, 2019; 133: 117–126.
- [14] Mende S, Peter M, Bartels K, Dong T T, Rohm H, Jaros D. Concentration dependent effects of dextran on the physical properties of acid milk gels. *Carbohydrate Polymers*, 2013; 98(2): 1389–1396.
- [15] Daniloski D, McCarthy N A, Gazi I, Vasiljevic T. Rheological and structural properties of acid-induced milk gels as a function of  $\beta$ -casein phenotype. *Food Hydrocolloids*, 2022; 131: 107846.
- [16] Liu D S, Zhou P, Nicolai T. Effect of Kapp.carrageenan on acid-induced gelation of whey protein aggregates. Part I: Potentiometric titration, rheology and turbidity. *Food Hydrocolloids*, 2020; 102: 105589.
- [17] Bi C H, Li D, Wang L J, Gao F, Adhikari B. Effect of high shear homogenization on rheology, microstructure and fractal dimension of acid-induced SPI gels. *Journal of Food Engineering*, 2014; 126: 48–55.
- [18] Dille M J, Draget K I, Hattrem M N. 9 - The effect of filler particles on the texture of food gels. In: *Modifying Food Texture*, Elsevier, 2015; pp.183–200.
- [19] Shi A M, Wang L J, Li D, Adhikari B. Characterization of starch films containing starch nanoparticles. Part 2: Viscoelasticity and creep properties. *Carbohydrate Polymers*, 2013; 96(2): 602–610.
- [20] Bi C H, Li D, Wang L J, Adhikari B. Effect of LBG on the gel properties of acid-induced SPI gels. *LWT*, 2017; 75: 1–8.